Gaussian solution of a charge-density-wave model

Federico Corberi
Dipartimento di Fisica, Università di Roma ''La Sapienza,'' Piazzale Aldo Moro 2, 00185 Rome, Italy
(Received 29 April 1996; revised manuscript received 1 October 1996)

We study the static and dynamic properties of the Fukuyama-Lee-Rice model for charge-density waves pinned by random impurities by means of a self-consistent Gaussian approximation. A depinning transition is observed, from an insulating to a conductive phase, when the external field E is raised above a critical value E_c, which depends both on the elastic coupling constant and on the disorder strength. The dynamics are characterized by an early stage followed by a crossover to an asymptotic regime. In the depinned phase a stationary periodic state is attained for long times characterized by a scaling behavior of the average current J, namely, $J \sim (E-E_c)^{\omega}$, with $\omega = 0.497 \pm 0.004$. [S0163-1829(97)03508-X]

I. INTRODUCTION

The static and dynamic properties of charge-density waves (CDW) pinned by random impurity potentials and under the influence of an applied external field have attracted a great deal of interest from theorists and experimentalists alike. This is mainly due to the very rich phenomenology observed in real materials such as $NbSe_3$ (Ref. 1) and $K_{0.30}MoO_3$ (Ref. 2) which has been successfully reproduced by Ginzburg-Landau-type Hamiltonian models. The phase diagram of these systems consists of an insulating, low field, pinned phase separated from a non-Ohmic conductive region by a field-induced phase transition. The insulating region shows several properties that are usually observed in glassy systems such as hysteresis, stretched exponential relaxation, and a highly degenerated number of metastable states. The conductive phase is characterized by long time transients, narrow-band and broadband noise, mode locking, and memory effects.

The most widely used model for the dynamics of this system has been that of Fukuyama, Lee, and Rice[3] describing an elastically deformable CDW pinned by random impurities. This results in the following equation of motion:

$$\frac{\partial \psi(\mathbf{x},t)}{\partial t} = B\nabla^2 \psi(\mathbf{x},t) - \sin[\psi(\mathbf{x},t) + \eta(\mathbf{x})] + E \qquad (1)$$

for the field $\psi(\mathbf{x},t)$, where B is an elastic coupling constant, E is the applied electric field, and $\eta(\mathbf{x})$ is a quenched white noise which takes into account the stochasticity of the impurity distribution. An overall analysis of the features of Eq. (1) has proven to be a hard task in both the theoretical and the numerical respect. Analytical difficulties arise mainly because of the presence of many interacting spatial modes[4] and of many metastable solutions below the threshold field. Simulations, on the other hand, can be extremely time consuming, especially in the region close to the sliding threshold, and they have been studied mainly in one dimension.[5,9,14]

In this paper we study the Fukuyama-Lee-Rice (FLR) model by means of a self-consistent Gaussian approximation (GA) or Hartree approximation, which allows one to write down closed-form equations for the main observables, namely, the polarization and the field correlation functions, by means of a self-consistency prescription which formally linearizes the problem. This widely used technique of statistical mechanics, well suited for Ginzburg-Landau models, has also been used in the study of order growth in an Ising system quenched below the critical line. In that case the shortcomings of this approximation are due to the remarkable difference between the exact field distribution, which is peaked around a couple of free energy minima, and the Gaussian approximant. In the case of the CDW model the method is more powerful because, due to the presence of an infinite number of potential minima, each of which is randomly shifted by the quenched noise $\eta(\mathbf{x})$, a Gaussian distribution is expected to be, at least qualitatively, adequate. In Fig. 1 the outcomes of a numerical simulation of Eq. (1) are presented, showing that the GA can be considered rather

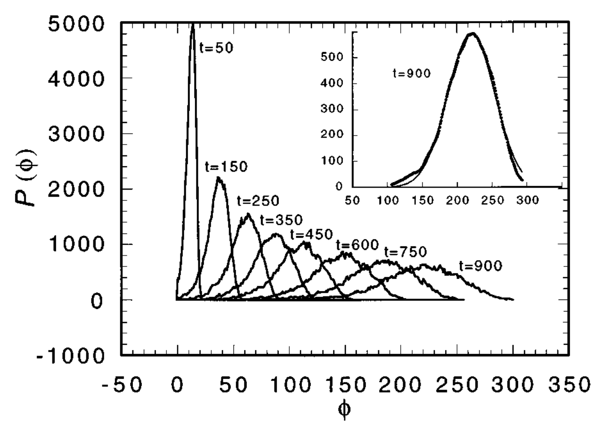

FIG. 1. The probability distribution $\mathcal{P}(\phi)$ obtained by numerical integration of the FLR model, Eq. (1), in the depinned phase ($B=0.5$, $E=0.6$, and $\sigma=10$) over a 10^5 lattice in $d=1$ is plotted at different times t. The figure suggests that, in this region, the GA is at least qualitatively correct. The quantity $\mathcal{P}(\phi)$ calculated in the late time regime ($t=900$) is shown in more detail in the inset, where a comparison is made with a Gaussian fit (continuous line). Apart from the tails of the distribution, where probably finite size effects become sensible, one observes general, good agreement between the data and their Gaussian interpolation. In the pinned phase, due to the presence of more complicated correlations, the agreement with the GA is less satisfactory.

satisfactory for the description of the depinned dynamics. In the pinned region, close to the threshold field for sliding, the GA is probably less reliable.

This paper is divided in five sections. In Sec. II the GA is introduced for the study of the static and dynamic properties of CDW. In Sec. III the equilibrium properties of the system are computed in the framework of the Hartree approximation and the calculation of the threshold field is discussed. In Sec. IV the dynamics of the model is studied both in the pinned and in the depinned phase. In Sec. V we summarize the results and discuss some conclusions.

II. GAUSSIAN APPROXIMATION

We assume the following probability distribution for the shifted field $\phi(\mathbf{x},t)=\psi(\mathbf{x},t)+\eta(\mathbf{x})$ at time t:

$$\mathcal{P}\{\phi\}=\frac{[\det C^{-1}(\mathbf{k},t)]^{1/2}}{(2\pi)^{d/2}}\times\exp\left\{-\frac{1}{2}\int_{|k|<\Lambda}d^dk[\phi(\mathbf{k},t)-P(t)]C^{-1}(\mathbf{k},t)\times[\phi(\mathbf{k},t)-P(t)]\right\},\tag{2}$$

where Λ is a high momentum phenomenological cutoff, $P(t)=\langle\phi(\mathbf{x},t)\rangle$ is the polarization,

$$C(\mathbf{k},t)=\langle\phi(\mathbf{k},t)\phi(-\mathbf{k},t)\rangle-P^2(t)\delta(\mathbf{k}),\tag{3}$$

the so-called structure factor, is the Fourier transform of the real space equal time pair connected correlation function

$$\mathcal{C}(\mathbf{r},t)=\langle\phi(\mathbf{x},t)\phi(\mathbf{x}+\mathbf{r},t)\rangle-P^2(t),\tag{4}$$

and the operator $\langle\,\rangle$ represents an average with respect to the distribution (2), namely, $\langle g\{\phi\}\rangle=\int\mathcal{D}\phi\, g\{\phi\}\mathcal{P}\{\phi\}$, where $g\{\phi\}$ is a generic function. We specify the quenched field $\eta(\mathbf{x})$ to be Gaussianly distributed with expectations

$$\langle\eta(\mathbf{x})\rangle=0\tag{5}$$

and

$$\langle\eta(\mathbf{x})\eta(\mathbf{x}+\mathbf{r})\rangle=\sigma\delta(\mathbf{r}).\tag{6}$$

From Eq. (1) the governing equation for $P(t)$ is obtained as

$$\frac{dP(t)}{dt}=f[P(t),S(t)]+E,\tag{7}$$

where

$$f[P(t),S(t)]=\langle\sin\phi(\mathbf{x},t)\rangle=e^{-S(t)/2}\sin P(t)\tag{8}$$

and $S(t)=\langle\phi^2(\mathbf{x},t)\rangle-P^2(t)$ is the averaged squared field fluctuation. This quantity must be evaluated self-consistently through the equation of motion for the structure factor $C(\mathbf{k},t)$ through

$$S(t)=\int_{|k|<\Lambda}\frac{d\mathbf{k}}{(2\pi)^d}\,C(\mathbf{k},t).\tag{9}$$

Transforming Eq. (1) into reciprocal space we obtain

$$\frac{\partial C(\mathbf{k},t)}{\partial t}=-2\{Bk^2+h[P(t),S(t)]\}C(\mathbf{k},t)+2Bk^2G(\mathbf{k},t),\tag{10}$$

where we have defined the cross correlation $G(\mathbf{k},t)=\langle\phi(\mathbf{k},t)\eta(-\mathbf{k})\rangle$ and the quantity $h[P(t),S(t)]$ is defined through[6]

$$\langle\phi(\mathbf{x}+\mathbf{r},t)\sin\phi(\mathbf{x},t)\rangle-P(t)\,\frac{dP(t)}{dt}=h[P(t),S(t)]\mathcal{C}(\mathbf{r},t),\tag{11}$$

with

$$h[P(t),S(t)]=e^{-S(t)/2}\cos P(t).\tag{12}$$

The equation of motion for $G(\mathbf{k},t)$ can be deduced from Eq. (1), as for $C(\mathbf{k},t)$; we obtain

$$\frac{\partial G(\mathbf{k},t)}{\partial t}=-\{Bk^2+h[P(t),S(t)]\}G(\mathbf{k},t)+Bk^2\sigma.\tag{13}$$

Equations (7), (10), and (13) constitute the governing integro-differential equations describing the static and dynamic behavior of the FLR model in the present Gaussian approximation. Experimental works on CDW (Refs. 1 and 2) as well as numerical analysis based on the FLR model usually probe the properties of the system by considering the behavior of the polarization current $J(t)=dP(t)/dt$ together with the correlation function

$$\mathcal{D}(\mathbf{r},t)=\langle\psi(\mathbf{x},t)\psi(\mathbf{x}+\mathbf{r},t)\rangle-P^2(t).\tag{14}$$

The Fourier transform $D(\mathbf{k},t)$ of this quantity can be related to $C(\mathbf{k},t)$ and $G(\mathbf{k},t)$ through $D(\mathbf{k},t)=C(\mathbf{k},t)-2G(\mathbf{k},t)+\sigma$.

In a previous paper[7] the behavior of CDW has been studied in the large-N limit (spherical model). Usually the large-N equations are closely related to those of the dynamical Hartree approximation. This happens because when the local potential is an algebraic polynomial of the order parameter field (the Ginzburg-Landau potential, for instance) one simply averages each term over the Gaussian distribution employing Wick's theorem. Due to fluctuations this procedure produces a renormalization of a finite number of coefficients. In the present case, however, since the pinning potential is a transcendent function, infinitely many terms are renormalized, leading to a radically different form of the linearized potential as compared to the large-N model equations. More precisely the GA causes an exponential $S(t)$ dependence of the amplitude of the trigonometric potentials $f[P(t),S(t)]$ and $h[P(t),S(t)]$ in Eqs. (7), (10), and (13) whereas in the large-N model $S(t)$ appears mainly like a phase in the trigonometric functions. The role of fluctuations is then very different in the two cases. In the large-N limit fluctuations are irrelevant in the vicinity of the critical field for sliding whereas in the GA they play a central role in the determination of the threshold field and of the dynamics. These differences, which will be stressed further in the following sections, arise because, although both the theories are Gaussian at all times, the physics which is described is radically different: in the large-N model, due to the presence of the $O(N)$ symmetry, the CDW essentially flows down the valleys of the potential; in the GA the order parameter is scalar and the CDW is interested by a barrier dynamics, as we shall see, which is much more realistic with respect to the original FLR model. As will be shown in Sec IV (see also Fig. 5) the very presence of barriers causes strong distortions of the CDW, because the system is not allowed to cross the barriers by rigid translation; for this reason fluctuations turn out to play a relevant role in the vicinity of the critical field whereas their importance is negligible in the $O(N)$ model, thus determining different physical properties.

III. STATICS

We consider the behavior of Eqs. (7), (10), and (13) studying, first, the static properties of the model. By setting equal to zero the left-hand sides of Eqs. (7), (10), and (13) we obtain

$$\sin P(\infty) = -\frac{E}{e^{-S(\infty)/2}} \tag{15}$$

and

$$C(\mathbf{k},\infty) = \frac{\sigma B^2 k^4}{[Bk^2 + e^{-S(\infty)/2}\cos P(\infty)]^2}. \tag{16}$$

Enforcing Eq. (9) we arrive at the self-consistency condition

$$S(\infty) = \sigma B^2 \int_{|k|<\Lambda} \frac{d\mathbf{k}}{(2\pi)^d} \frac{k^4}{[Bk^2 + \sqrt{e^{-S(\infty)} - E^2}]^2}. \tag{17}$$

Equation (17) does not admit solution for E larger than a critical value $E_c(B,\sigma)$, as will be clear below; hence $E = E_c(B,\sigma)$ is the threshold field for sliding. Below $E_c(B,\sigma)$ the CDW relaxes to the static equilibrium configuration while above $E_c(B,\sigma)$ it is depinned and slides. For B or σ sufficiently small $S(\infty) \simeq 0$. Hence the critical field is determined by the singularity of the integrand at $E_c^2(B,\sigma) = \exp[-S(\infty)] = 1$. In the large-$B$ limit, instead, by neglecting $\sqrt{e^{-S(\infty)} - E^2}$ with respect to BK^2 in Eq. (17) we find $S(\infty) \to c\sigma$, with $c = \Lambda/(2\pi)^d$. Proceeding as before we obtain $E_c(B,\sigma) \simeq \exp[-(c/2)\sigma]$. This result should be compared with the one found in Ref. 8, where a similar calculation has been employed. In Ref. 8 it is argued, supported by a comparison with the values of E_c derived by direct computer simulation of Eq. (1), that the GA allows one to accurately calculate the threshold field for small values of the coupling constant B. In Fig. 2(a) the critical field determined by Eq. (17) is shown as a function of B for different values of σ in $d=1$. In Fig. 2(b) a comparison is presented between the determination of $E_c(B,\sigma)$ obtained by direct numerical simulation of Eq. (1) and the result of the GA in the case $\sigma = 1$. The comparison shows, in agreement with Ref. 8, that the GA is reliable in the strong pinning region (small B), which corresponds to small fluctuations of the field. For weak pinning (large B) $S(\infty)$ is large and the Gaussian ansatz for the fluctuations is less accurate, because in this limit $E_c(B,\sigma)$ should go to zero.

The results of this section illustrate the profound differences between the large-N limit and the GA for CDW. In the spherical model the fluctuations turn out to be irrelevant at the critical point; this occurs because in the vicinity of the critical point one is allowed to neglect $S(t)$ with respect to $P(\infty)$ in the self-consistency equation because $P(t)$ diverges approaching E_c and $S(\infty)$ is finite. As a result the critical field turns out to be independent both of B and of σ, because these parameters determine the weight of fluctuations, and one finds $E_c \equiv 1$. In the present approach, due to the structure of the self-consistency equation, $S(t)$ always produces finite corrections from the trivial value $E_c = 1$, which corresponds to $B=0$ (or $\sigma=0$). The physical origin of this mathematical property is the following: when the quenched disorder is stored into the system the energy of the CDW is minimized by an adequate compromise between pinning and elastic energies. Since B and σ determine the relative strength of these two contributions, equilibrium properties depend continuously on these parameters, and so E_c. One can easily convince oneself by inspection of Eq. (17) that $S(\infty)$ is a monotonously increasing function of σ for fixed B. Hence, as the the disorder increases, the CDW gets more and more scattered among many minima of the local potential. One could expect that the GA breaks down when the fluctuation

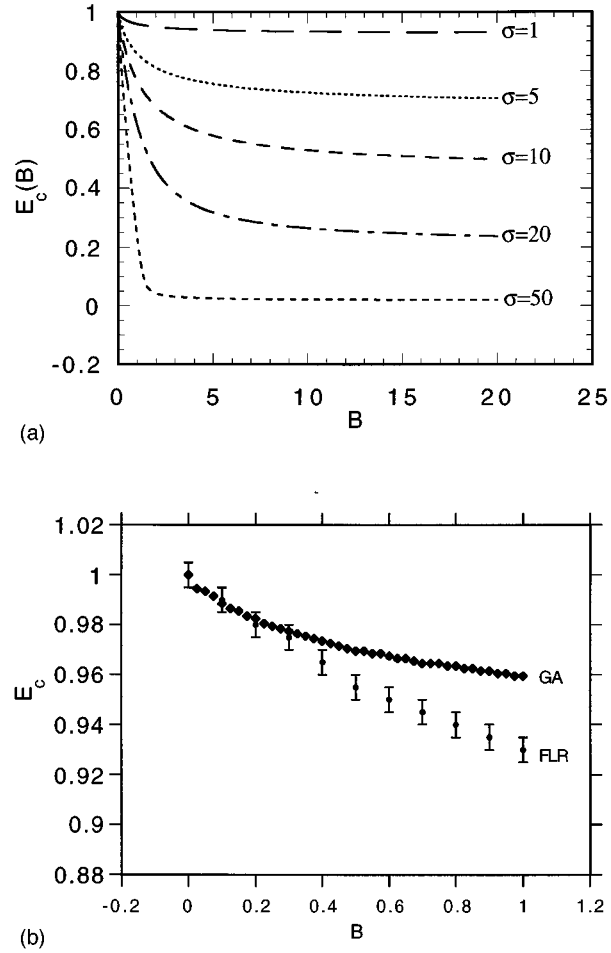

FIG. 2. In (a) the threshold field $E_c(B,\sigma)$ determined from Eq. (17) is plotted against B for different values of the disorder strength σ. In (b) the comparison is made between a numerical determination of $E_c(B,\sigma)$ obtained by direct computer simulation of Eq. (1) on a one-dimensional 10^3 point mesh with lattice constant $a = 2\pi$ (points with error bars) and the results of the GA (heavy dots), in the case $\sigma = 1$. The figure shows good agreement in the strong pinning regime (small B).

of the FLR equation grows too much with respect to the GA. The fact that, in this approach, $S(\infty)$ grows with the disorder strength suggests that the GA is reliable in the region $\sigma B \ll 1$.

IV. DYNAMICS

In this section we study the dynamics of the model. In order to characterize the dynamical process we need to specify the initial configuration of the field $\phi(\mathbf{x},0)$. In the following we will consider an uncorrelated initial condition characterized by $C(\mathbf{k},0)=\Delta$ and $G(\mathbf{k},0)=0$; the initial value of the polarization $P(0)$ is not very relevant: since the model is invariant under 2π rigid translations this variable is always near to one of the equilibrium values of the pinned phase. On the other hand, $S(0)$ can be, depending on Δ, very far from equilibrium. In this case an early stage is observed, which can be rather long, followed by a crossover to an asymptotic regime characterized by the relaxation of the system already near equilibrium. In the conductive phase a similar situation may occur since, although $P(t)$ grows indefinitely, $S(t)$ attains, for long times, a stationary solution characterized by periodic oscillations around a mean value $\overline{S}$. In this phase an early stage can be required, depending on the initial condition, to bring S close to $\overline{S}$. Then the late stage is entered. If $S(0) \gg S(\infty)$ [or $S(0) \gg \overline{S}$ in the conductive region], since the fluctuations of the field are large, the effective strength of the pinning potential is averaged to zero and the CDW is free to slide under the influence of the external field alone. By neglecting $f[P(t),S(t)]$ with respect to E we find

$$P(t) \simeq Et \tag{18}$$

in the early stage. From Eq. (10), neglecting $h[P(t),S(t)]$ with respect to Bk^2 and $G(\mathbf{k},t)$ with respect to $C(\mathbf{k},t)$, by virtue of the initial condition, we obtain

$$S(t) \sim \frac{(Bt)^{-d/2}}{\Delta}. \tag{19}$$

As Fig. 3 shows, these considerations apply to both the pinned and the depinned phase. In this time domain the CDW behaves as a simple elastic string driven by the external field E because the elastic energy stored in the system by the initial condition prevails over the local potential. As time passes and $S(t)$ approaches its asymptotic value, the effect of the pinning potential becomes gradually more relevant and a different regime is observed which is characterized by an oscillatory behavior of $S(t)$ around a mean value which is still decaying. In this time domain the system still tries to dissipate elastic energy by reducing fluctuations [i.e., $S(t)$] but, differently from the very early stage, in order to cross barriers it is forced to deform periodically in time. This oscillatory behavior, which is enhanced by the quenched randomness strength σ, is very reminiscent of the depinned motion which is observed asymptotically for $E>E_c$ (see also Fig. 5) and will be further discussed below. As $S(t) \simeq S(\infty)$ the CDW enters the asymptotic regime which is characterized by a complex balancing between the external field and the potential terms. In the insulating phase the system gets trapped around one local minimum and an exponential relaxation of both $P(t)$ and $S(t)$ towards the equilibrium values $P(\infty),S(\infty)$ is found. Equation (7), in fact, admits the

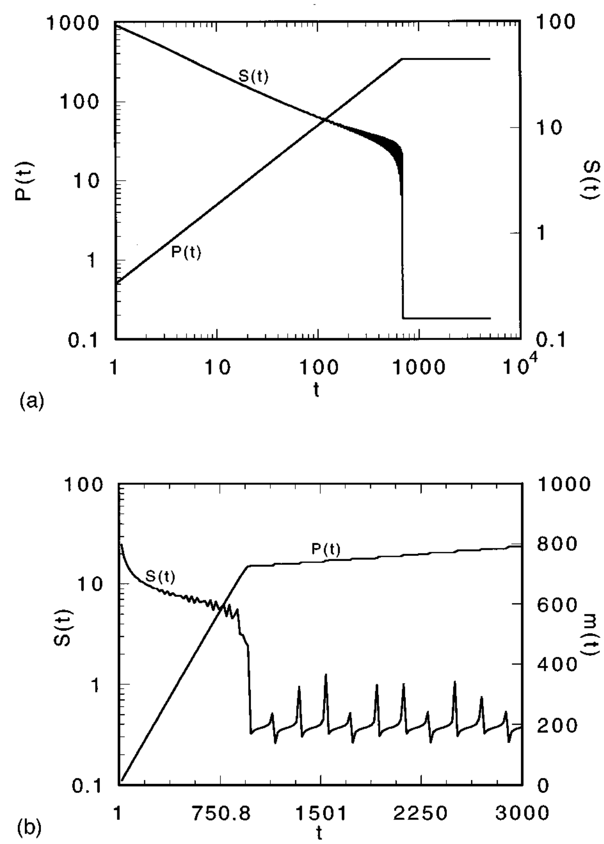

FIG. 3. The behavior of $P(t)$ and of $S(t)$ is plotted. In (a) the evolution of these quantities is shown in the pinned region ($B=1$, $E=0.5$, $\sigma=5$, and $d=1$). An early regime is evident, characterized by $P(t)=Et$ and $S(t) \sim (Bt)^{-d/2}/\Delta$, followed by an exponential relaxation to the equilibrium configuration. Between these two regimes an intermediate behavior can be observed that is characterized by periodic oscillations of $S(t)$ that widen until the system gets trapped around one local minimum. In (b) the same quantities are shown in the depinned region ($B=1$, $E=0.772$, $\sigma=5$, and $d=1$). After an early and an intermediate regime analogous to the one observed in the insulating region a stationary periodic state is reached that is characterized by a staircase growth of $P(t)$ and an oscillating behavior of $S(t)$.

asymptotic solution $P(\infty)-P(t) \sim S(\infty)-S(t) \sim \exp(-bt)$ where b is a constant. Above threshold a stationary state is attained which is characterized by periodic oscillations of $S(t)$ and $J(t)$ around their mean values $\overline{S}$ and $\overline{J}$ [see Fig. 2(b)]. In the critical region above threshold [$E \simeq E_c(B,\sigma)$] a numerical integration of Eqs. (7), (10), and (13) yields

$$\overline{J} \sim [E-E_c(B,\sigma)]^{\omega}, \tag{20}$$

with a value of the exponent ω which is compatible with $\omega=\frac{1}{2}$ with good accuracy in any dimension d ($\omega=0.497 \pm 0.004$ in $d=1$; see Fig. 4). For $E \gg E_c$, on the other hand, the local potential can be neglected in Eq. (7) and $\omega=1$. In Fig. 4 $\overline{J}$ is plotted against E in the critical region above E_c for $d=1$. The same result, $\omega=\frac{1}{2}$, is predicted by simple one-particle models[11] and by the large-N limit solution.[7] The mean field result of $\omega=\frac{3}{2}$ (Ref. 12) has led to the expectation that the CDW model with many interacting degrees of freedom would show $\omega \neq \frac{1}{2}$. The analytical work of Parisi and Pietronero[13] on a coarse-grained version of the FLR model

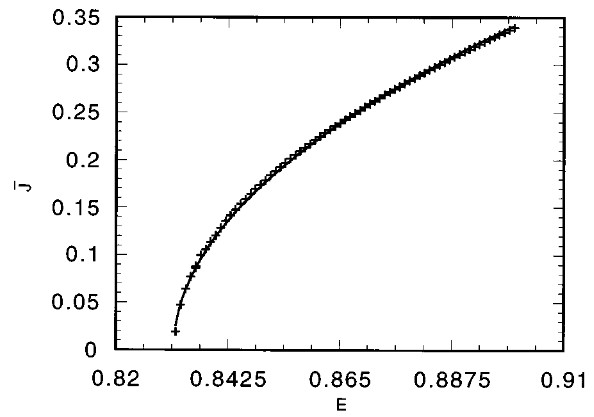

FIG. 4. The average current $\overline{J}$ is plotted against E for $B=1$ and $\sigma=\pi^2/3$ in $d=1$. Crosses represent the results of the numerical integration of Eqs. (7), (10), and (13), while the continuous line describes the law $(E-E_c)^\omega$ with $\omega=0.497$.

leads to $\omega=1$ in every dimension d. Given the minuscule extent of the critical regime observed in most of the systems the prospect of conclusive evidence about this exponent coming either from numerical simulations or experiments on real systems appears unlikely. The result of this section shows that the same value of ω found in simple one-particle-type models (the large-N limit can also be considered to belong to this class of models since fluctuations are allowed but they are irrelevant at criticality) can also be obtained when many interacting degrees of freedom are taken into account, as in the present scheme, despite the fact that the physics described by the GA in the sliding region close to the threshold field is by far more complex than the one observed in single-coordinate models. To this purpose it is interesting to observe, in Fig. 5, the crossing mechanism of a barrier in the GA. Initially the CDW lies in a minimum of the local potential. The external field is not sufficient to produce a rigid translation of the CDW across the barrier; due to a favorable realization of the quenched noise $\eta(\mathbf{x})$, however, a small region of the CDW becomes locally depinned and crosses the potential maximum. This produces an avalanche effect, since the nearest neighbors are pulled through the barrier too, and there is a sudden increase of the fluctuation $S(t)$. The mechanism ends when the whole system reaches the next minimum. For large B or σ, since in this case S is large too, the behavior is similar but more complicated because the CDW is scattered among many minima. As Fig. 3 shows, an analogous behavior is also observed in an intermediate stage of the dynamics before the system gets trapped into a local minimum for $E<E_c$ or attains the stationary state for $E>E_c$. This somewhat complex character of the dynamics which is captured by the GA, however, does not produce any appreciable difference in the velocity exponent ω with respect to its single-particle value. On the other hand, our determination disagrees violently with the mean field result $\omega=\frac{3}{2}$, suggesting that our approach, although mean field in spirit, is radically different from that of Ref. 12 when dynamical properties are considered.

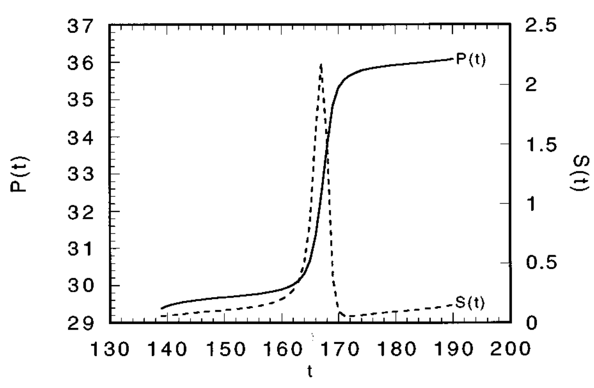

FIG. 5. The crossing mechanism of a barrier is shown in the depinned phase ($B=1$, $E=0.95$, $\sigma=1$, and $d=1$).

V. CONCLUSIONS

In this paper we have studied the dynamic Hartree approximation for CDW. This analytical scheme allows one to compute the static and dynamic properties of the original CDW model in a relatively simple way. The approximation is quite satisfactory and reproduces several properties of the original model such as the presence of a depinning transition at a critical value of the applied field $E_c(B,\sigma)$ which depends both on the elastic coupling constant B and on the disorder strength σ. In the depinned region the critical behavior is described by the scaling law (20), with ω consistent with $\omega=\frac{1}{2}$ in every dimension, for the polarization current. Accurate numerical determinations of this exponent in CDW models are quite difficult due to the smallness of the critical region and because the crossover to the high field behavior, $\omega=1$, is so gradual that one can be misled by a simple straight line on a log-log plot of the current. Analogous difficulties are also encountered in the numerical simulation of an automaton model for CDW introduced by Myers and Sethna.[9] Their analysis yields $\omega=0.45\pm0.05$ in $d=1$, which is in excellent agreement with the prediction of the GA, and slightly larger values of this exponent in higher dimensions where their results probably suffer from the inability to go to large enough linear system sizes to resolve the critical regime, as observed by the authors themselves. Direct numerical simulations[10,14] of Eq. (1) report slightly larger values of this exponent.

In the present approach the correlations are taken into account at an elementary level, allowing one to compute the threshold field and the depinned dynamics with good accuracy in the strong pinning regime $\sigma B\ll 1$. From the inspection of Fig. 1 no significant deviations from Gaussianity are observed when the system is depinned, suggesting that our results relative to the conductive phase are reliable. It would be interesting to know, by a more extensive and systematic numerical analysis, whether $\mathcal{P}(\phi)$ is effectively Gaussian, because, in that case, our results are exact. On the other hand, the method is not as suitable for studying the behavior of CDW in the critical region below $E_c(B,\sigma)$, where complicated strongly non-Gaussian correlations set in.

As a final comment let us add that in the same scheme it is possible to take simply into account the effect of thermal noise.

ACKNOWLEDGMENT

We are grateful to U. Marini Bettolo Marconi for discussions and for a critical reading of the manuscript.

[1] P. Monceau, N. P. Ong, and A. M. Portis, Phys. Rev. Lett. **37**, 602 (1976); R. M. Fleming, D. E. Moncton, and D. B. McWhan, Phys. Rev. B **18**, 5560 (1978); R. E. Thorne, W. G. Lyons, J. W. Lyding, and J. R. Tucker, *ibid*. **35**, 6348 (1987).

[2] J. Dumas, C. Schlenker, J. Marcus, and R. Buder, Phys. Rev. Lett. **50**, 757 (1983); G. Kriza and G. Mihály, *ibid*. **56**, 2529 (1986).

[3] H. Fukuyama and P. A. Lee, Phys. Rev. B **17**, 535 (1977); P. A. Lee and T. M. Rice, *ibid*. **19**, 3970 (1979).

[4] L. Sneddon, M. C. Cross, and D. S. Fisher, Phys. Rev. Lett. **49**, 292 (1982); L. Sneddon, *ibid*. **52**, 65 (1984); S. N. Coppersmith and P. B. Littlewood, Phys. Rev. B **31**, 4049 (1985); M. V. Feigel'man and V. M. Vinokur, Phys. Lett. **87A**, 53 (1981).

[5] P. B. Littlewood, in *Charge Density Waves in Solids*, edited by L. P. Gor'kov and G. Gruner (Elsevier, New York, 1989), and references therein; A. A. Middleton and D. S. Fisher, Phys. Rev. Lett. **66**, 92 (1990); A. Erzan, A. Veermans, R. Heijungs, and L. Pietronero, Phys. Rev. B **41**, 11 522 (1990); Physica A **166**, 447 (1990).

[6] The function $h[P(t),S(t)]$, which is defined through Eq. (11), can be easily obtained from $f[P(t),S(t)]$, enforcing the relation $h[P(t),S(t)]=df[P(t),S(t)]/dP(t)$, which can be proved directly deriving, with respect to $P(t)$, the functional integral that defines $f[P(t),S(t)]$. The same result can also be obtained by making a Taylor expansion of the sine and taking the average of each term using Wick's theorem. The resulting series is readily recognized to be the Taylor expansion of the function $h[P(t),S(t)]$ defined via Eq. (12).

[7] F. Corberi and U. Marini Bettolo Marconi, Physica A **225**, 281 (1996).

[8] L. Pietronero and M. Versteeg, Physica A **179**, 1 (1991).

[9] C. R. Myers and J. P. Sethna, Phys. Rev. B **47**, 11 171 (1993).

[10] L. Pietronero and S. Strassler, Phys. Rev. B **28**, 5863 (1983); L. Pietronero, in *Highlights of Condensed-Matter Theory*, edited by F. Bassani, F. Fermi, and M. P. Tosi (North-Holland, Amsterdam, 1985).

[11] G. Gruner, A. Zawadowski, and P. M. Chaikin, Phys. Rev. Lett. **46**, 511 (1981).

[12] D. S. Fisher, Phys. Rev. B **31**, 1396 (1985).

[13] G. Parisi and L. Pietronero, Europhys. Lett. **16**, 321 (1991); Physica A **179**, 16 (1991).

[14] P. Sibani and P. B. Littlewood, Phys. Rev. Lett. **64**, 1305 (1990).